High Spin States in Nuclei:

Exotic Quantal Rotation

I

Umesh Garg

University of Notre Dame

Supported in part by the National Science Foundation

CNSSS17

August 23-29, 2017

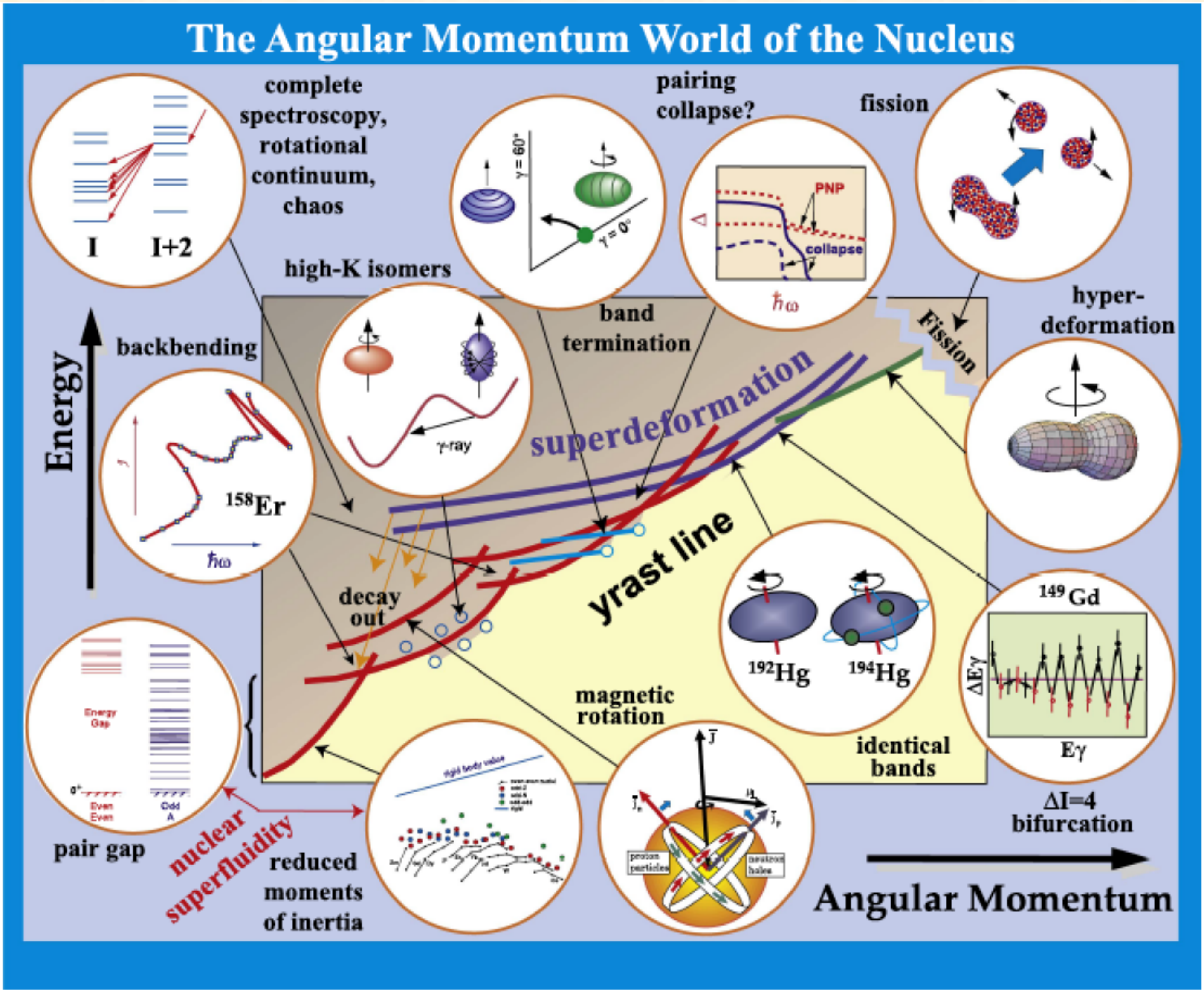

M. Riley *et al.*, Phys. Scr. 91, 123002 (2016)
adapted from W. Nazarewicz, Nucl. Phys. A **630**, 239c (1998).

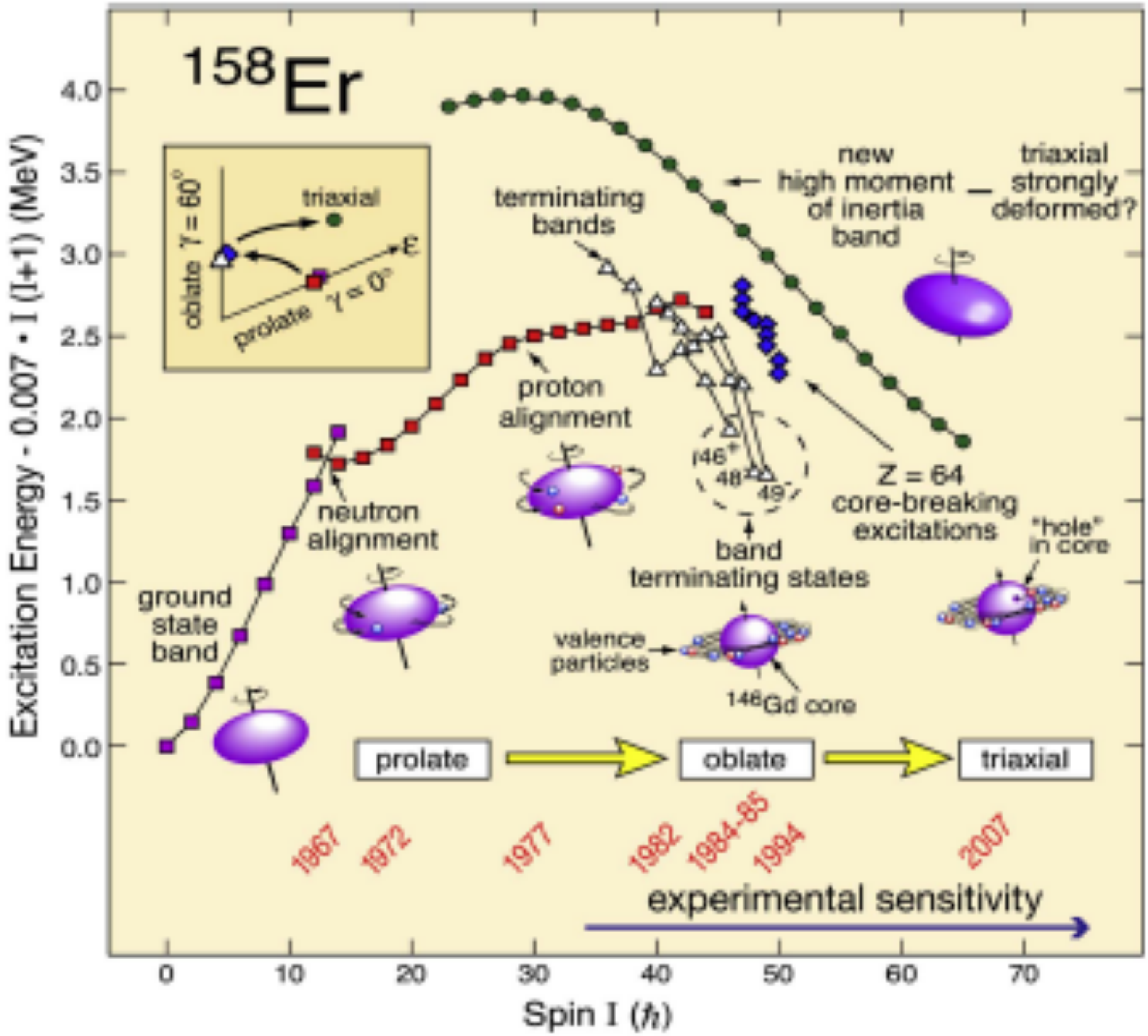

M. Riley *et al.*, Phys. Scr. 91, 123002 (2016)

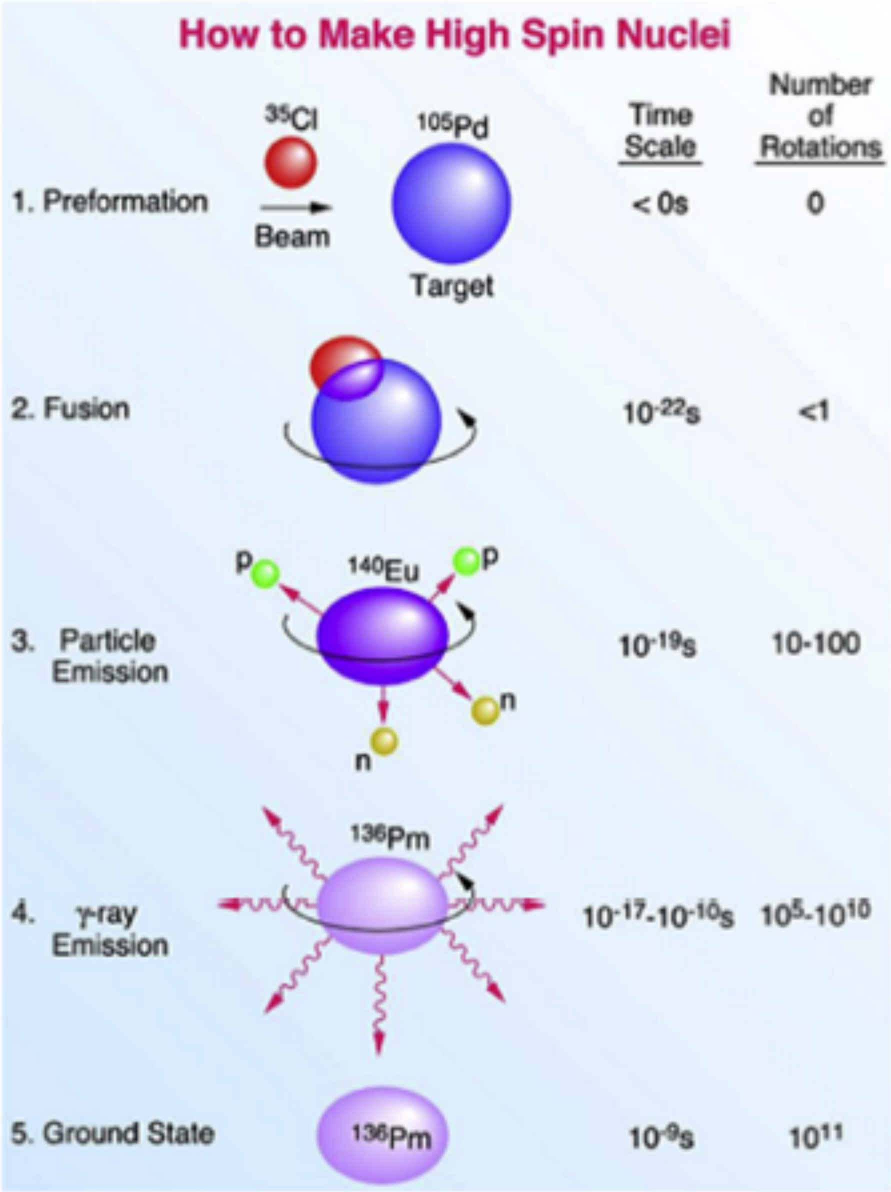

M. Riley *et al.*, Phys. Scr. 91, 123002 (2016)

Interaction of gamma-rays with matter

Photo effect

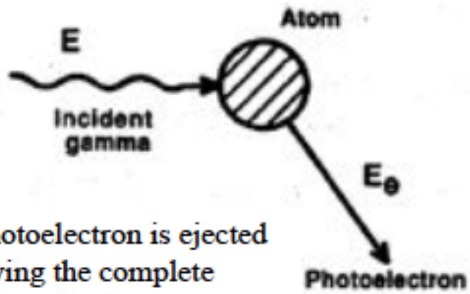

A photoelectron is ejected carrying the complete gamma-ray energy (- binding)

Compton scattering

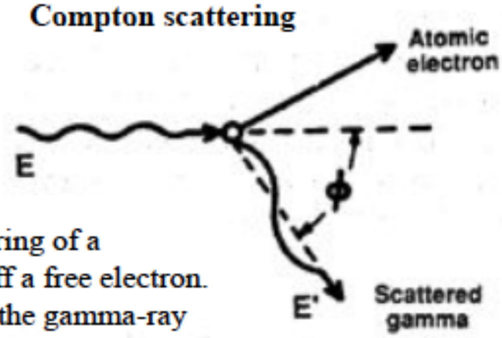

Elastic scattering of a gamma ray off a free electron.
A fraction of the gamma-ray energy is transferred to the Compton electron

Pair production

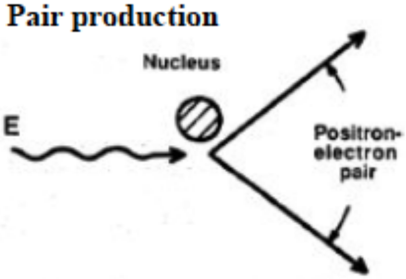

If gamma-ray energy is >> 2 $m_o c^2$ (electron rest mass 511 keV), a positron-electron can be formed in the strong Coulomb field of a nucleus. This pair carries the gamma-ray energy minus 2 $m_o c^2$.

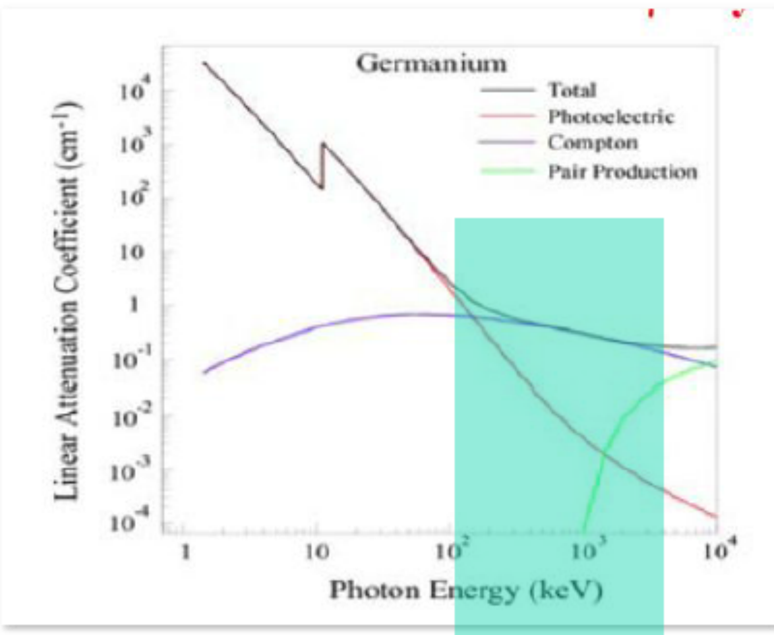

Photoelectric:
~ Z^{4-5}, $E_g^{-3.5}$

Compton:
~ Z, E_g^{-1}

Pair production:
~ Z^2, increase with E_g

Example; 1.33 MeV
5 interactions: 4 Compton, 1 photo
Separation of interactions: 0.5 – 5 cm

γ-ray detectors over the years:

- NaI (Tl)
- Ge(Li)
- 2 Ge(Li)s
- Hyperpure Ge
- Ge arrays
- Compton-suppressed Ge arrays

  Tessa, HIRA, OSIRIS, GASP,
  Argonne-Notre Dame γ-ray Facility

- Clover and Cluster Arrays

  Yrast Ball, Eurogam, INGA, CAGRA

- Tracking Arrays

  GRETINA, AGATA, GRETA

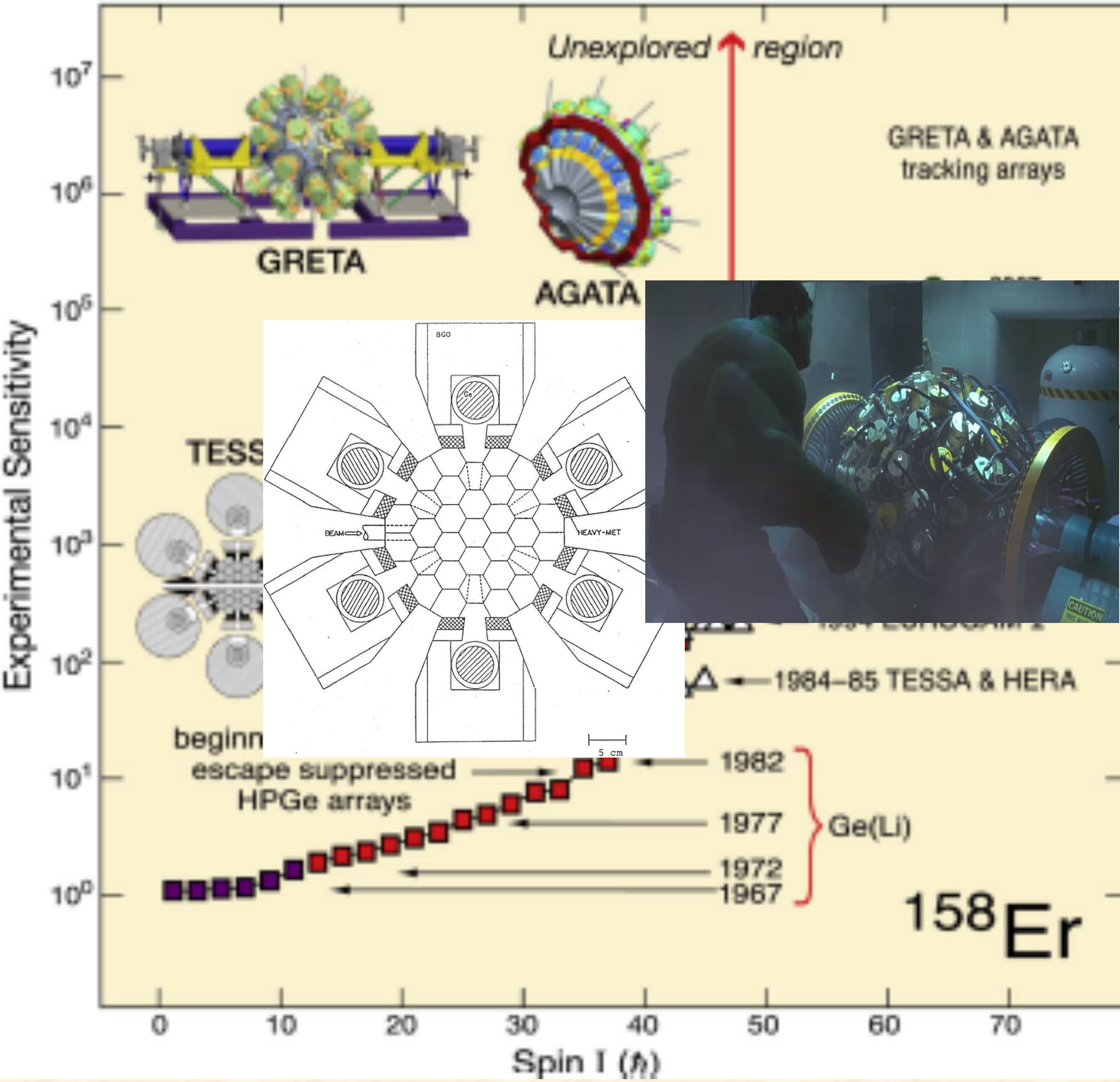

M. Riley *et al.*, Phys. Scr. 91, 123002 (2016)

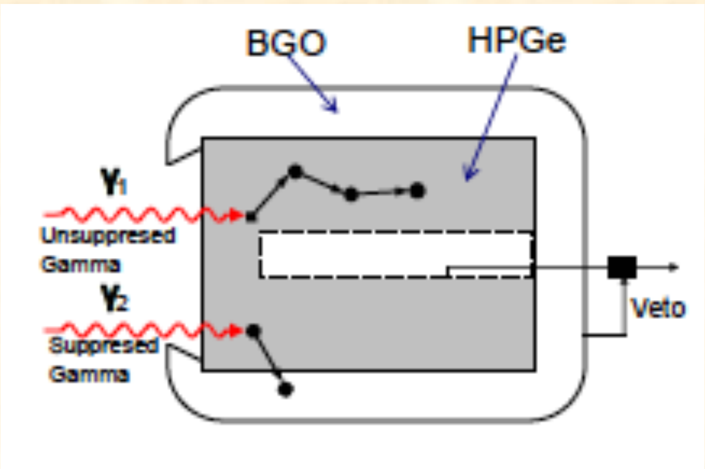
BGO
HPGe
γ1
Unsuppresed
Gamma
γ2
Suppresed
Gamma
Veto

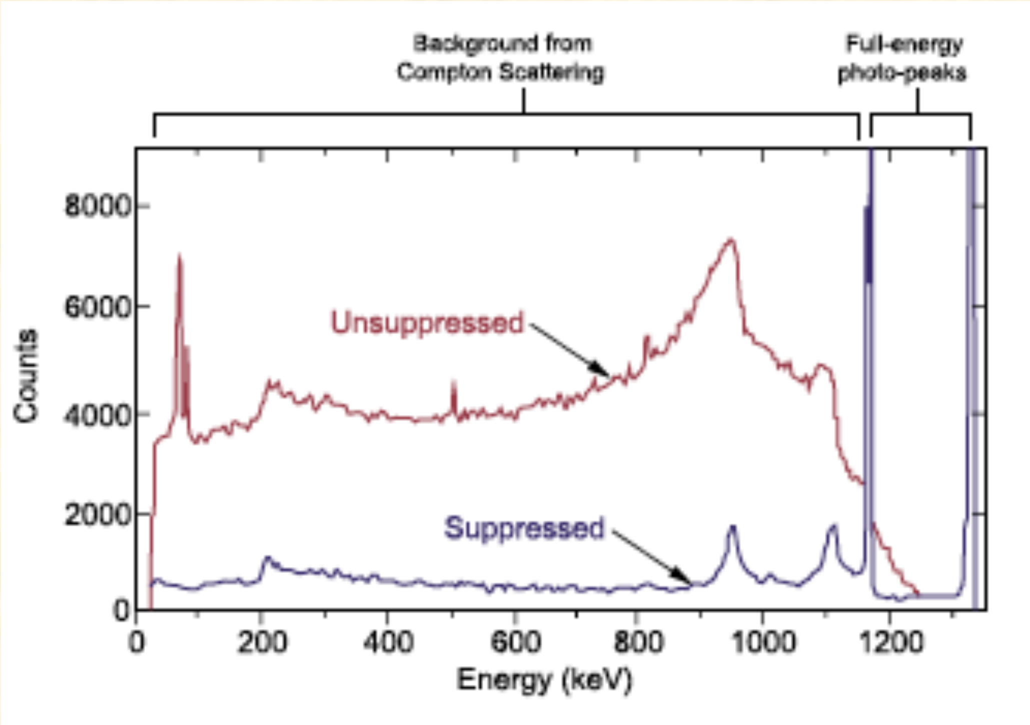
Background from
Compton Scattering
Full-energy
photo-peaks
Unsuppressed
Suppressed
Counts
Energy (keV)
0
2000
4000
6000
8000
0
200
400
600
800
1000
1200

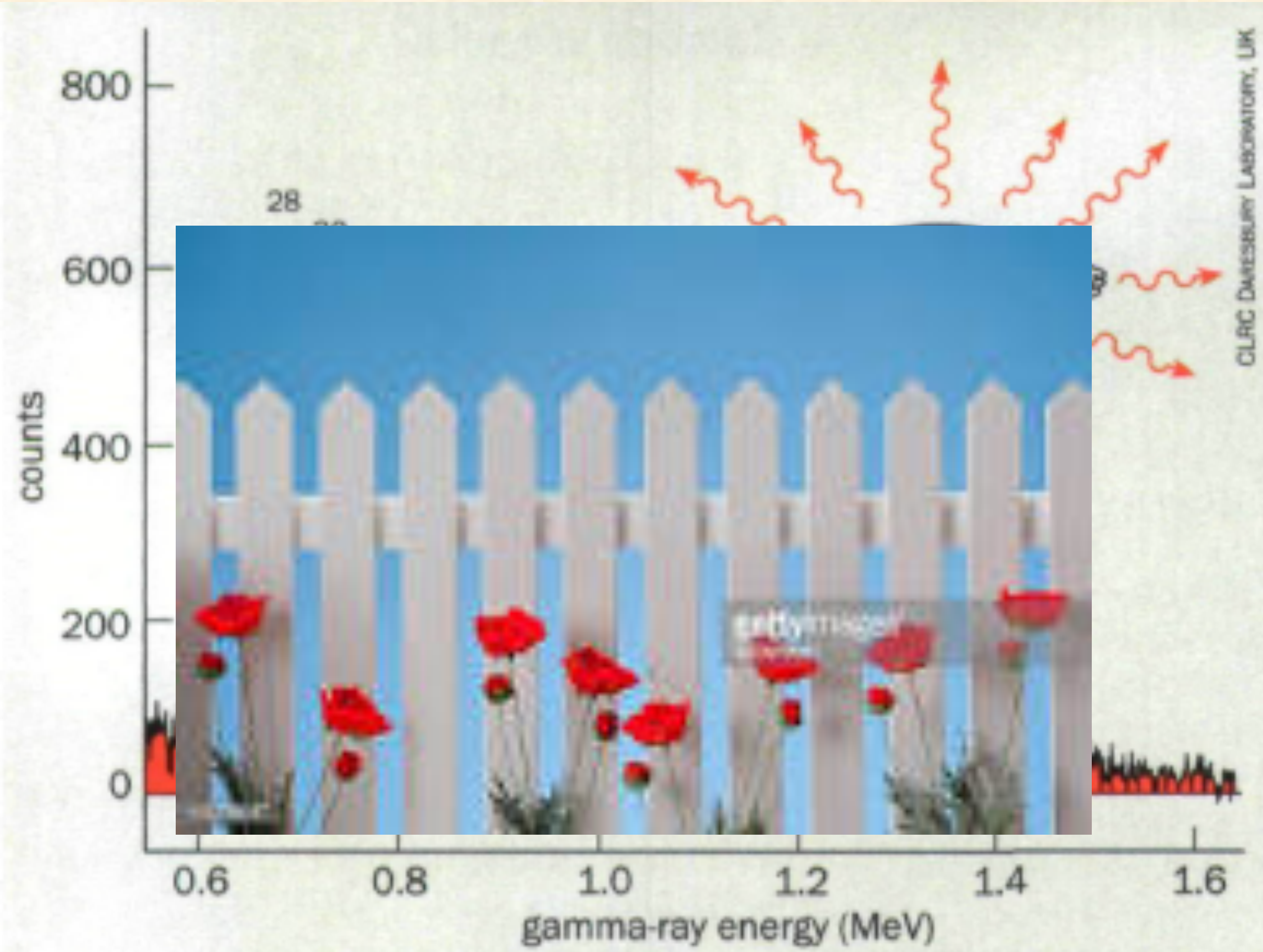

Superdeformed nuclei of dysprosium-152 decay by emitting a regular spectrum of gamma-rays. The number above each transition is the angular momentum quantum number, which decreases by two each time a photon is emitted. The photon carries $2\hbar$ of angular momentum away from the nucleus, which slows down the rotation. After emitting approximately 20 such gamma-rays the nucleus abruptly loses its deformation.

Clark and Wadsworth, *Physics Workd* **11(7),** 25 (1998).

VOLUME 63, NUMBER 4 PHYSICAL REVIEW LETTERS 24 JULY 1989

Observation of Superdeformation in ^{191}Hg

E. F. Moore, R. V. F. Janssens, R. R. Chasman, I. Ahmad, T. L. Khoo, and F. L. H. Wolfs
Argonne National Laboratory, Argonne, Illinois 60439

D. Ye, K. B. Beard, and U. Garg
University of Notre Dame, Notre Dame, Indiana 46556

M. W. Drigert
Idaho National Engineering Laboratory, EG&G Idaho Inc., Idaho Falls, Idaho 83415

Ph. Benet and Z. W. Grabowski
Purdue University, West Lafayette, Indiana 47907

J. A. Cizewski
Rutgers University, New Brunswick, New Jersey 08903
(Received 8 March 1989)

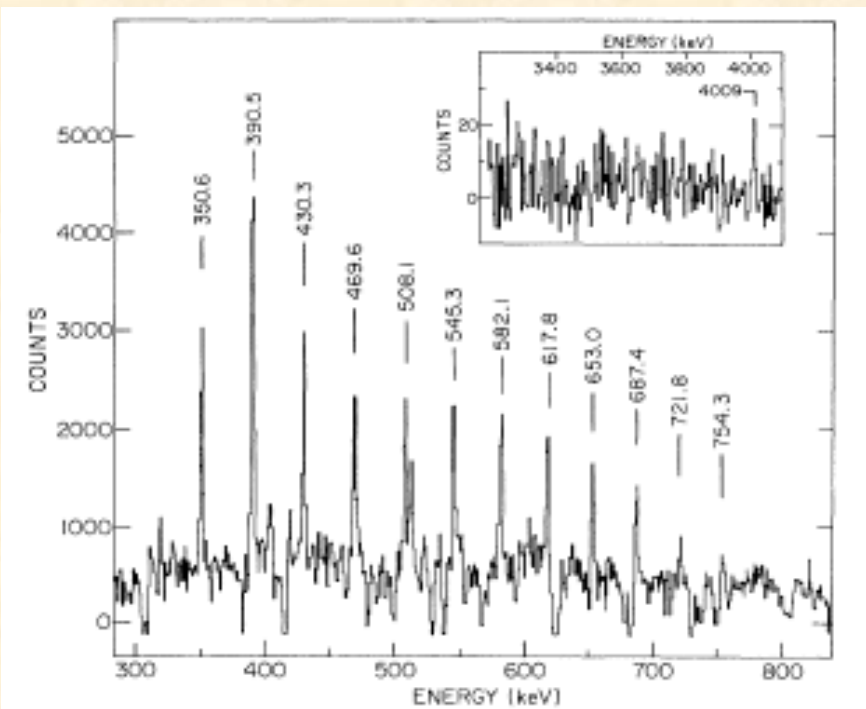

Effective Resolution: Doppler Broadening

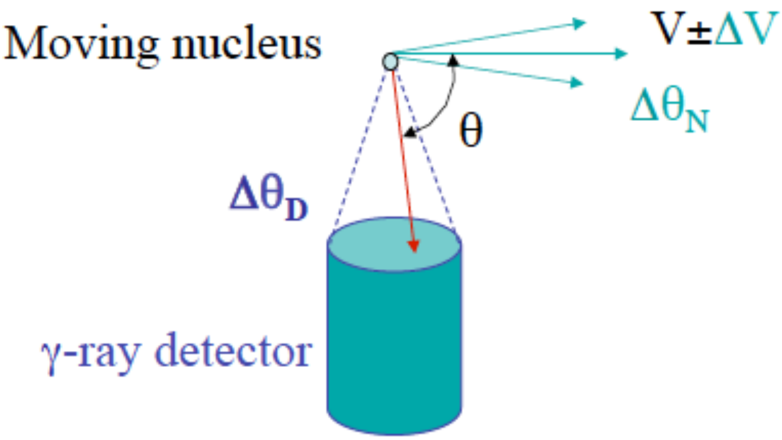

Doppler shift

$$E_\gamma = E_\gamma^0 \frac{\sqrt{1-\frac{V^2}{c^2}}}{1-\frac{V}{c}\cos\theta}$$

Broadening of detected gamma ray energy due to:

- Spread in speed ΔV
- Distribution in the direction of velocity $\Delta\theta_N$
- Detector opening angle $\Delta\theta_D$

➔ **Need accurate determination of V and θ.**

➔ Minimize opening angle and particle detector

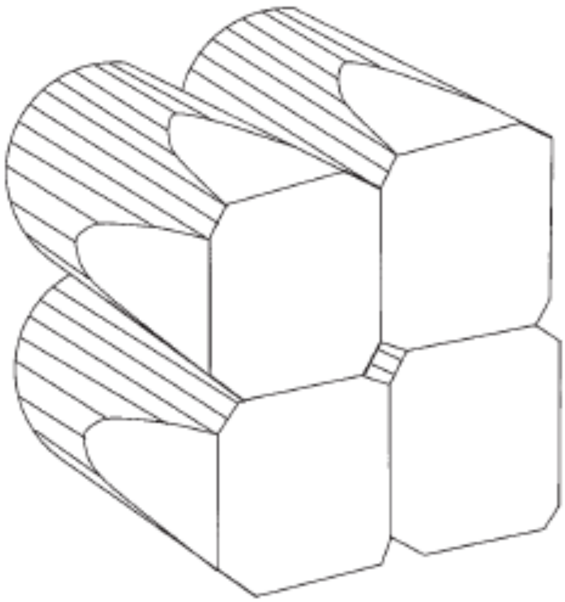

Figure 13. Schematic view of a clover detector.

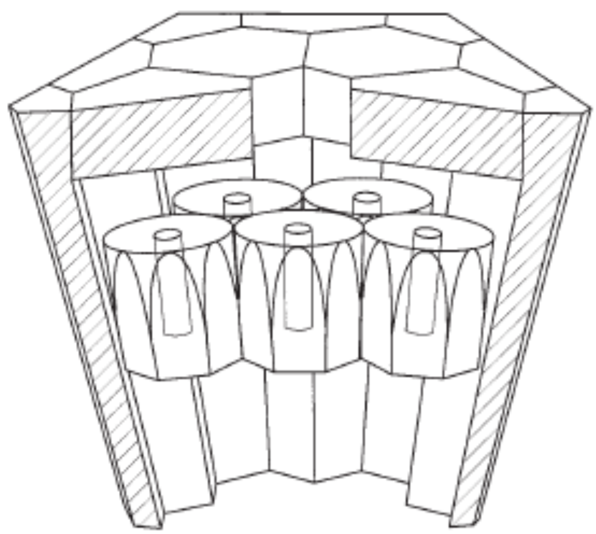

Figure 14. Schematic diagram (side view cross section) of a cluster of 7 HPGe detectors (5 visible) surrounded by their BGO Compton suppressor (hatched cross section).

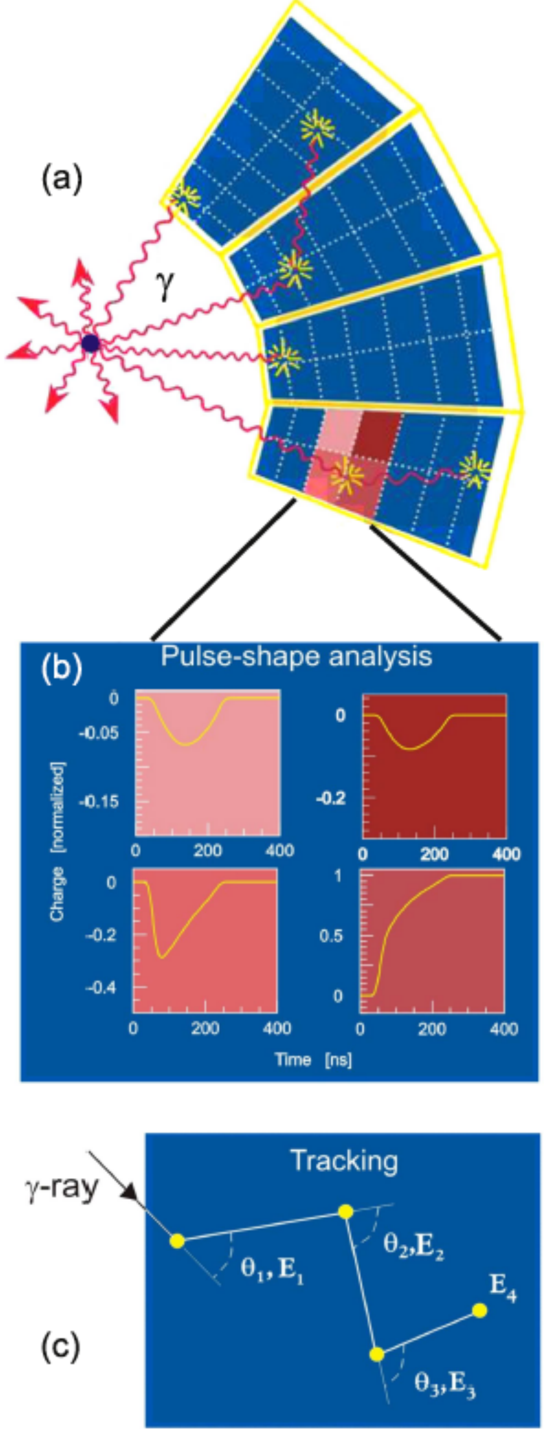

Figure 8. Gamma-ray tracking technique principles. (a) Tracking arrays will consist of a closed shell of segmented Ge detectors. (b) Analysis of the pulse-shapes of signals from segments containing the interaction(s), transient signals in adjacent segments will also be analysed, thus allowing the measurement of the three-dimensional locations of the interactions, and their energies. (c) Tracking algorithms, based on the physics of the underlying physical processes such as pair production and Compton scattering, are used to determine the scattering sequence and identify the separate interactions of the gamma rays.

M. Riley *et al.*

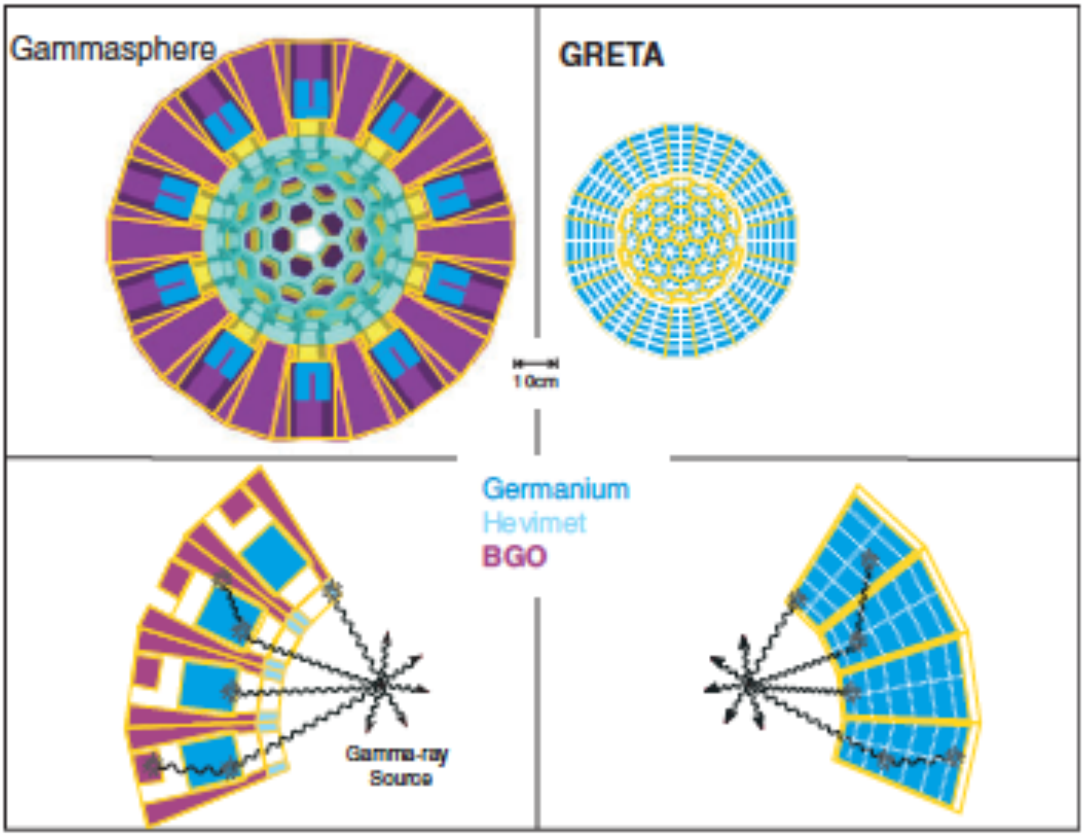

Figure 17. Comparison between the current state-of-the-art detector Gammasphere (left) and the proposed GRETA array (right). In the top part, both instruments are shown on the same scale. The lower portion (not to scale) indicates the two different approaches. While anti-Compton shields suppress cross scattering between Ge crystals and hevimet absorbers prevent direct hits of the shields and thereby false suppression, a γ ray tracking array accepts all γ rays, thereby significantly increasing the efficiency.

From I. Y. *Lee*

Position resolution

- Collimated beam of ^{137}Cs 663 keV
- Highest energy point from signal decomposition

singles

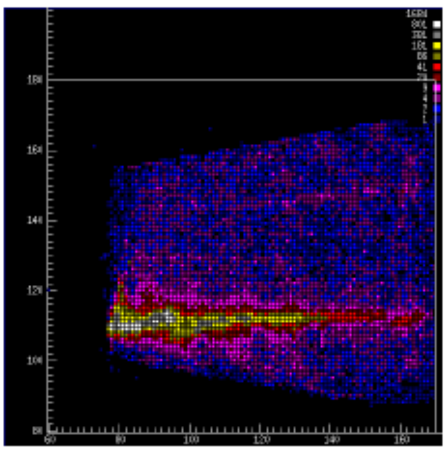

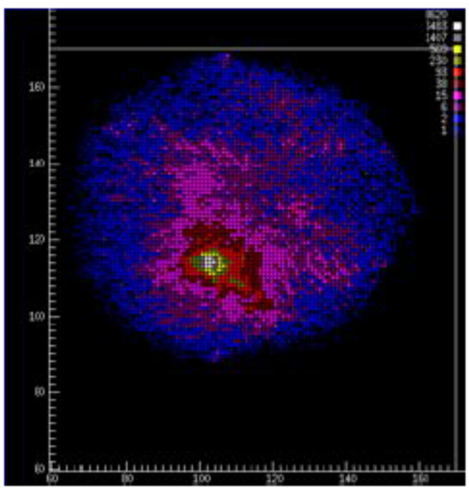

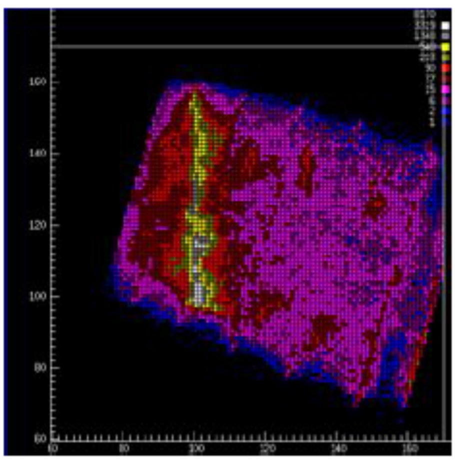

- $\sigma_{x,y,z} \sim 2$ mm

From I. Y. *Lee*

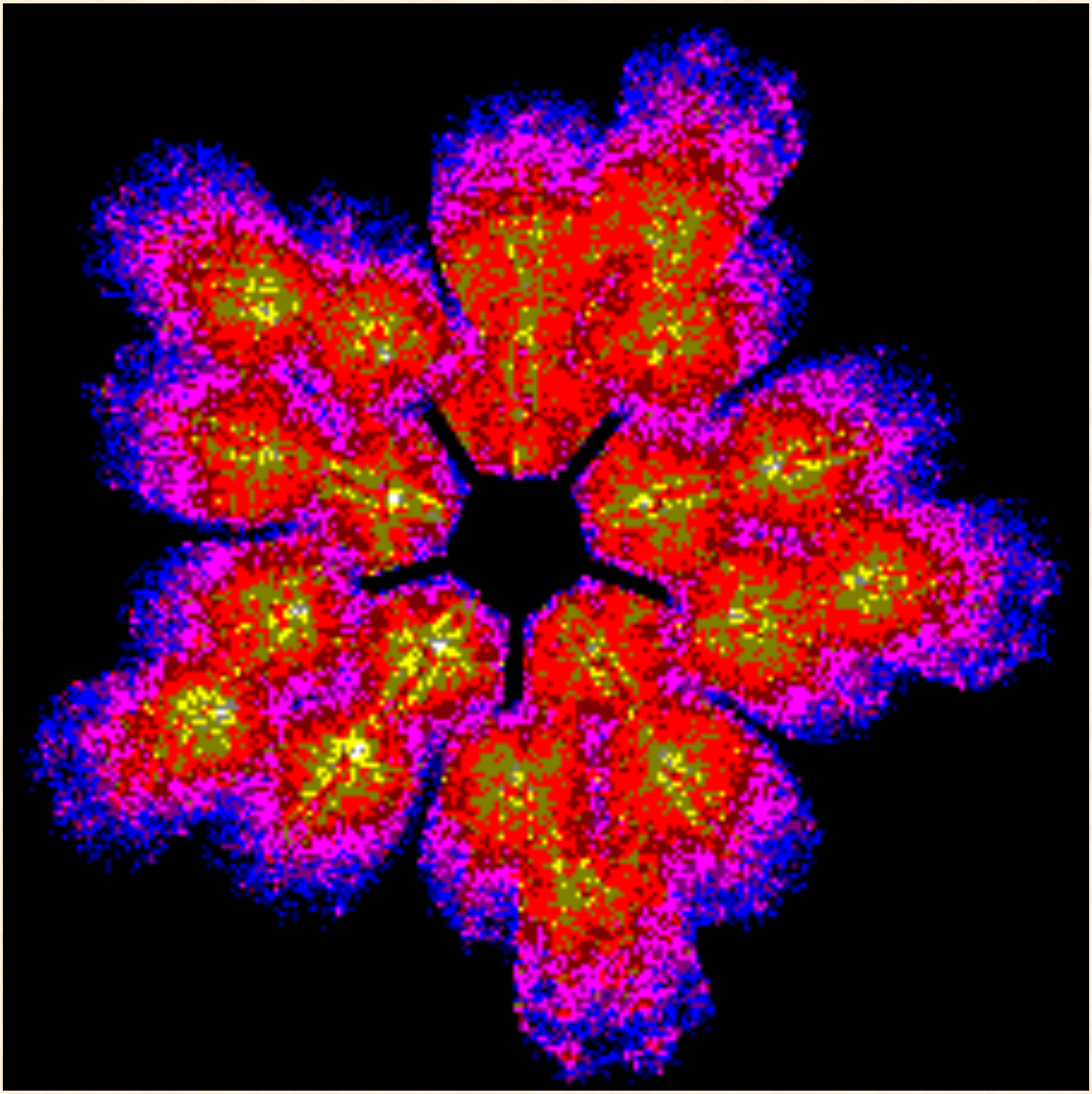

From I. Y. *Lee*

PRL **116,** 112503 (2016) PHYSICAL REVIEW LETTERS week ending 18 MARCH 2016

Direct Evidence of Octupole Deformation in Neutron-Rich ^{144}Ba

B. Bucher,[1,*] S. Zhu,[2] C. Y. Wu,[1] R. V. F. Janssens,[2] D. Cline,[3] A. B. Hayes,[3] M. Albers,[2] A. D. Ayangeakaa,[2] P. A. Butler,[4] C. M. Campbell,[5] M. P. Carpenter,[2] C. J. Chiara,[2,6,†] J. A. Clark,[2] H. L. Crawford,[7,‡] M. Cromaz,[5] H. M. David,[2,§] C. Dickerson,[2] E. T. Gregor,[8,9] J. Harker,[2,6] C. R. Hoffman,[2] B. P. Kay,[2] F. G. Kondev,[2] A. Korichi,[2,10] T. Lauritsen,[2] A. O. Macchiavelli,[5] R. C. Pardo,[2] A. Richard,[7] M. A. Riley,[11] G. Savard,[2] M. Scheck,[8,9] D. Seweryniak,[2] M. K. Smith,[12] R. Vondrasek,[2] and A. Wiens[5]

Excited states in the neutron-rich $N = 38, 36$ nuclei ^{60}Ti and ^{58}Ti were populated in nucleon-removal reactions from ^{61}V projectiles at 90 MeV/nucleon. The γ-ray transitions from such states in these Ti isotopes were detected with the advanced γ-ray tracking array GRETINA and were corrected event by event for large Doppler shifts ($v/c \sim 0.4$) using the γ-ray interaction points deduced from online signal decomposition. The new data indicate that a steep decrease in quadrupole collectivity occurs when moving from neutron-rich $N = 36, 38$ Fe and Cr toward the Ti and Ca isotones. In fact, ^{58,60}Ti provide some of the most neutron-rich benchmarks accessible today for calculations attempting to determine the structure of the potentially doubly magic nucleus ^{60}Ca.

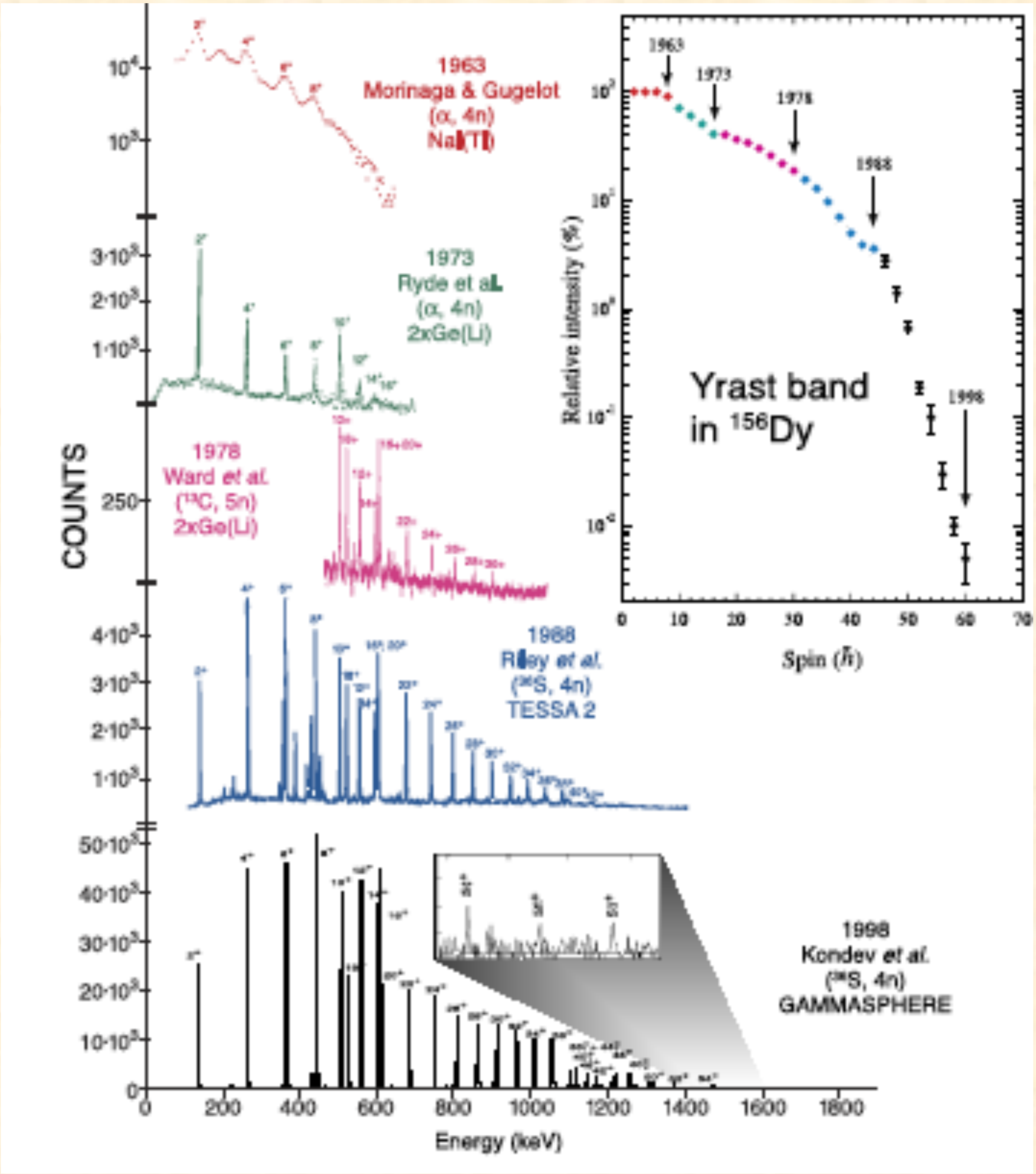

M. Riley *et al.*, Phys. Scr. 91, 123002 (2016)

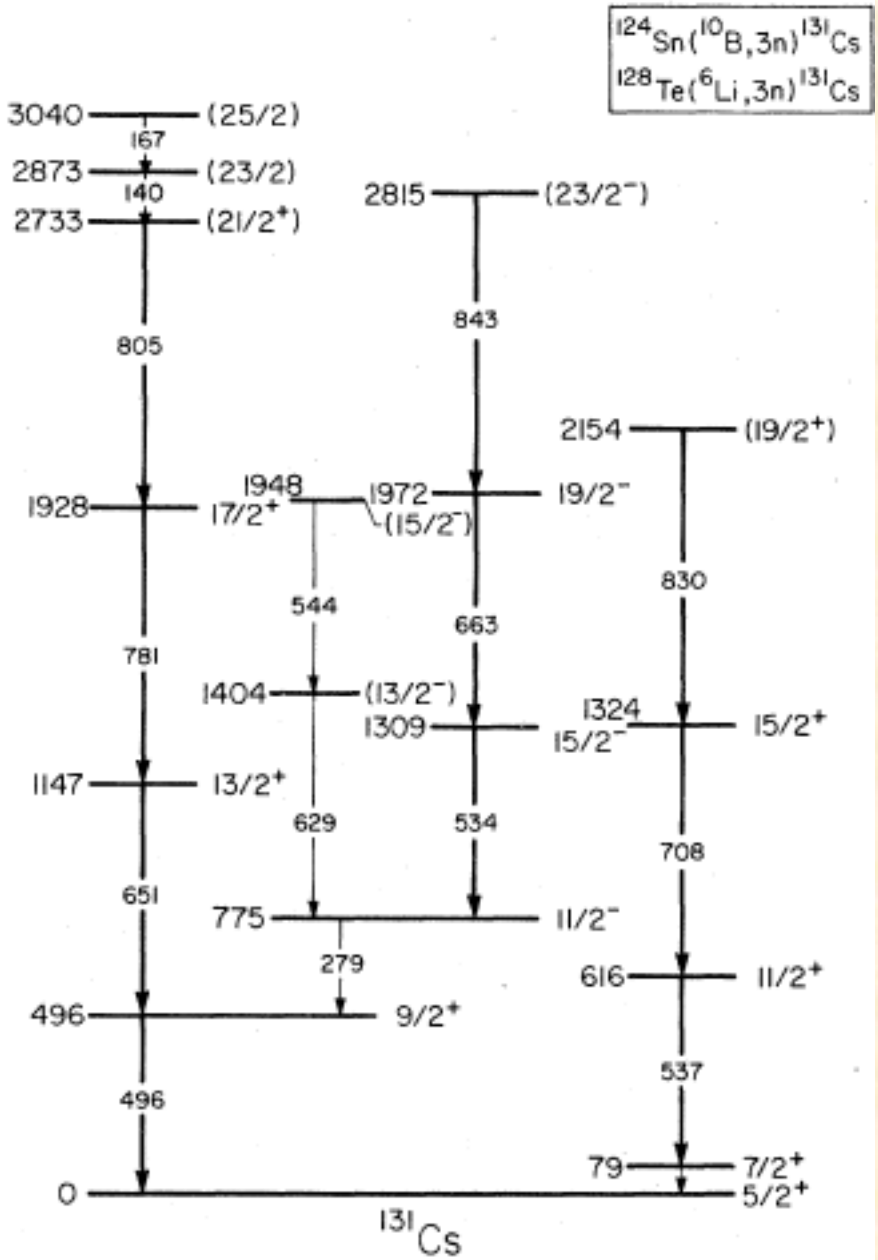

FIG. 5. Level scheme for ^{131}Cs extracted from the present work. All energies are in keV.

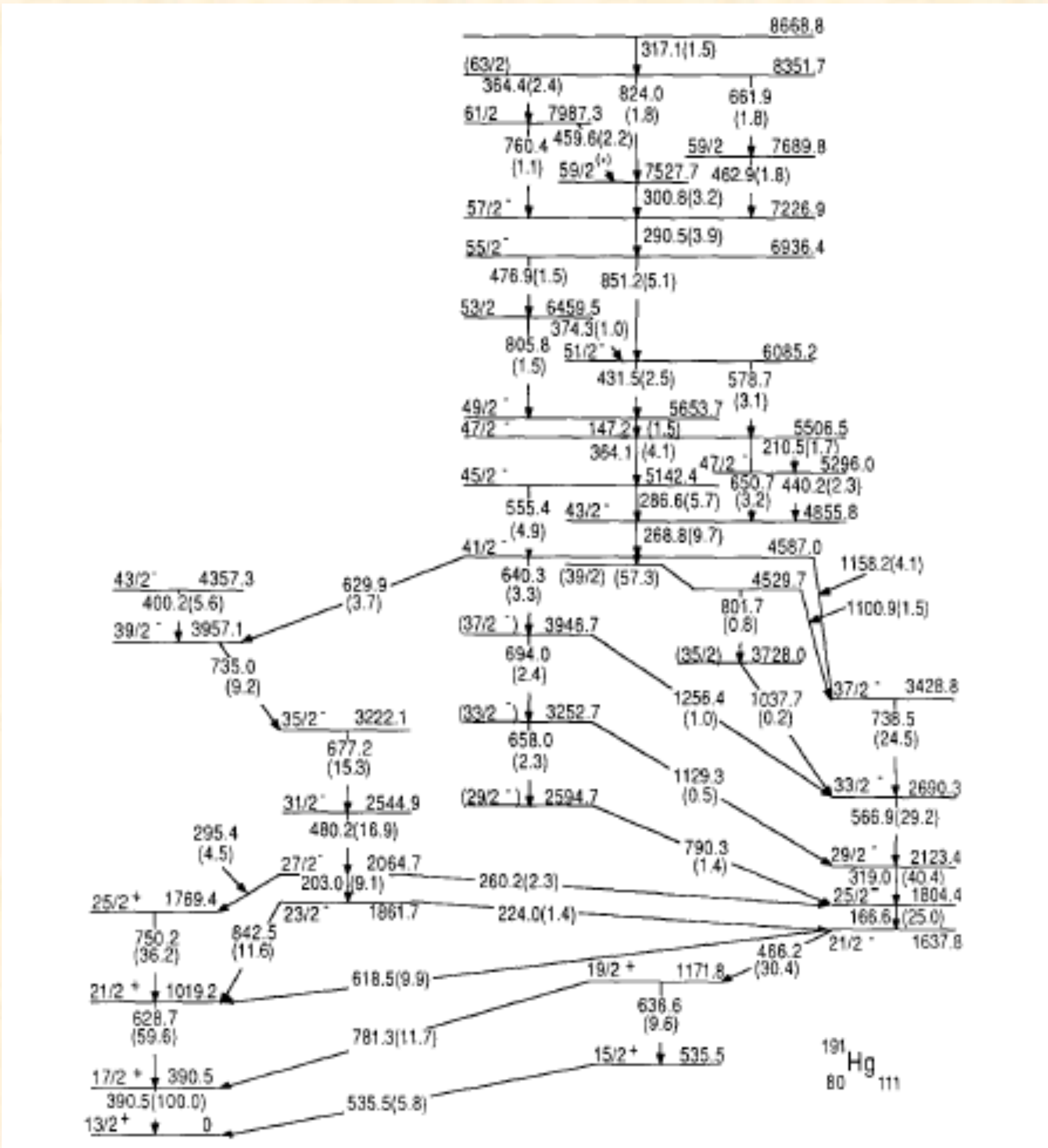

D, Ye *et al.* Phys. Lett. B **236**, 7 (1990) “standard” γ-ray spectroscopic measurements:

- γ–γ coincidences
- Angular Distributions/Correlations
- Lifetimes
- Linear Polarizations

◆ γ–γ coincidences

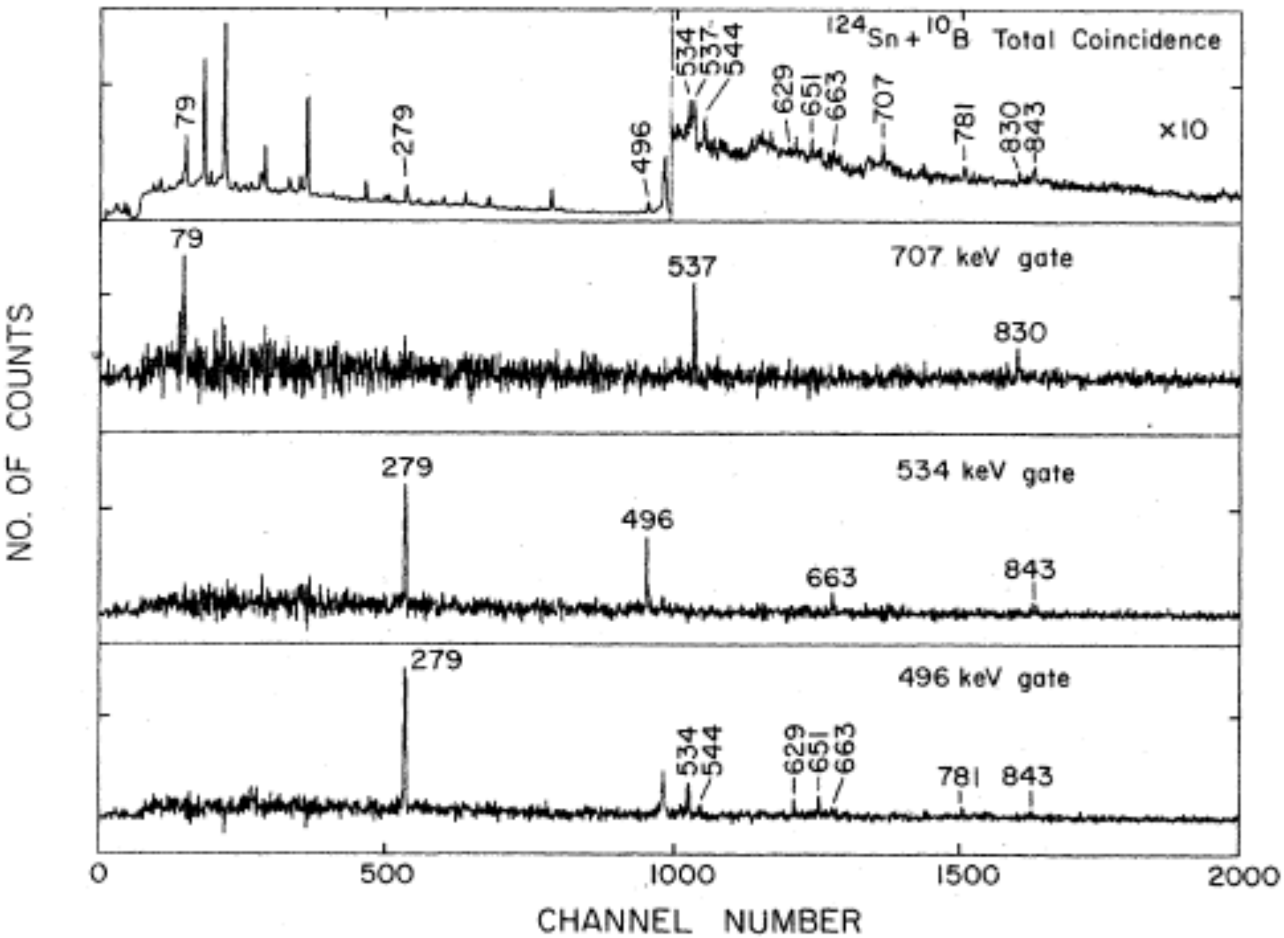

TABLE III. γ-γ coincidence results for ^{131}Cs.

E_γ (keV)	γ rays in coincidence[a]
140[b]	167, 496, 651, 781, 805
167[b]	140, (651), (781), (805)
279	496, 534, 544, 629, 663, (843)
496	279, 534, 544, 629, 651, 663, 781, (843), 140,[b] (167),[b] 805[b]
534	279, 496, 663, 843
537[c]	79, 115,[d] 707, 830
544	279, 496, 629
629	279, 496, 544
651	496, 781, 140,[b] 167[b]
663	279, 496, 534
707	79, 537, 830
781	496, 651, 140,[b] 167,[b] 805[b]
805[b]	140, (167), 496, 651, 781
830	79, 537, 707
843	279, (496), 534, (663)

[a] Parentheses denote weak coincidences.

[b] These γ rays are seen only in the $^{128}Te(^{6}Li, 3n)^{131}Cs$ reaction.

[c] Doublet.

[d] Not included in the level scheme.

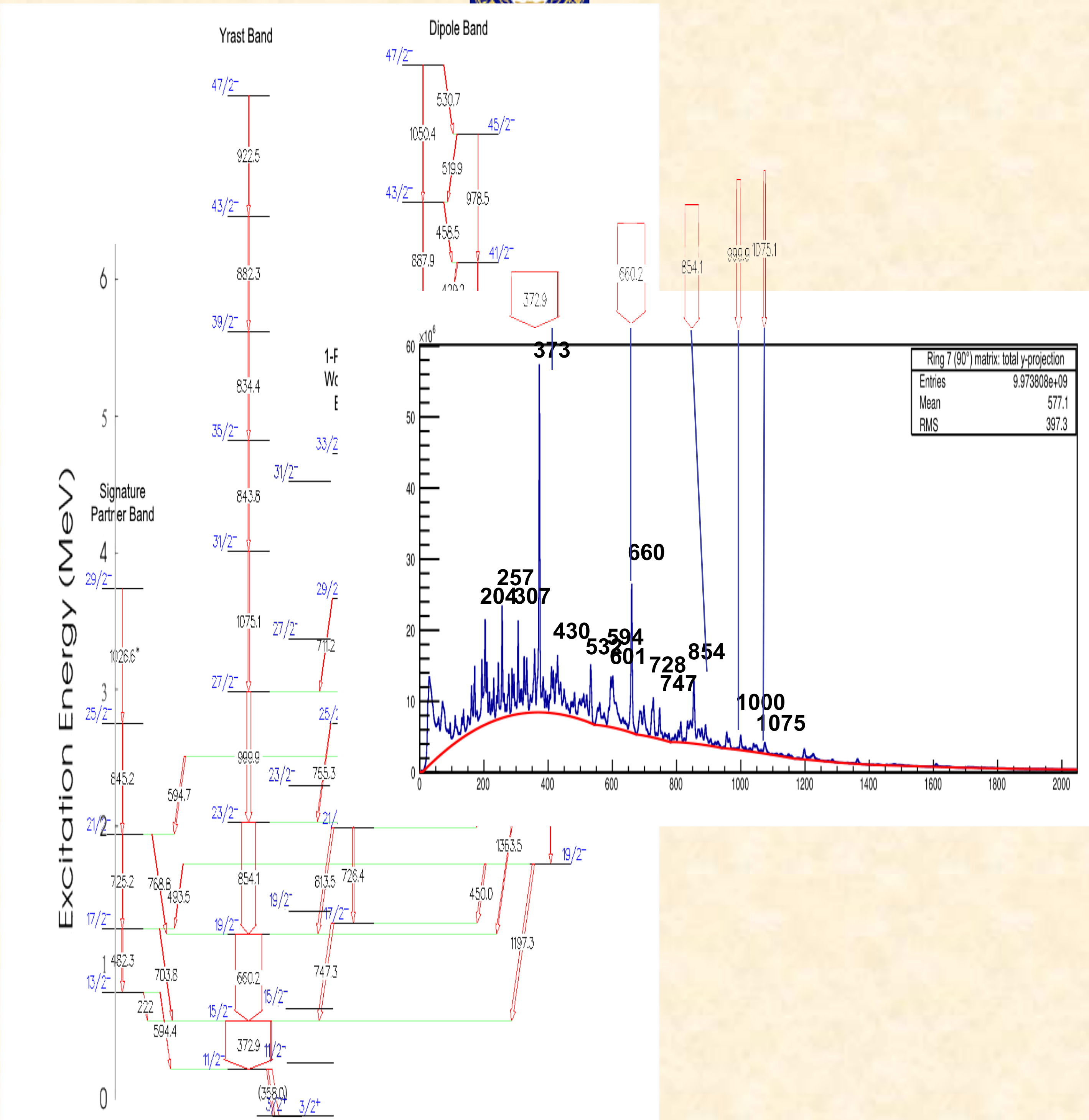

animations courtesy of T. McMaken

◆ Angular Distributions/Correlations

TABLE VI. Angular Distribution Results for ^{131}Cs.

E_{γ}^{a} (keV)	I_{γ}^{b}	A_2	A_4	Assignment
78.7[c]	>100			$7/2^+ \to 5/2^+$
1140.1	10	-0.30 ± 0.05	0.05 ± 0.07	$(23/2) \to (21/2)$
279.1	68	-0.22 ± 0.02	-0.04 ± 0.03	$11/2^- \to 9/2^+$
496.2	100	0.23 ± 0.02	-0.10 ± 0.03	$9/2^+ \to 5/2^+$
533.6	41	0.17 ± 0.06	-0.12 ± 0.07	$15/2^- \to 11/2^-$
536.7	55	0.20 ± 0.05	-0.03 ± 0.06	$11/2^+ \to 7/2^+$
543.9	11	-0.44 ± 0.04	-0.11 ± 0.08	$(15/2^-) \to (13/2^-)$
629.3	20	-0.56 ± 0.03	0.02 ± 0.04	$(13/2^-) \to 11/2^-$
651.1	22	0.30 ± 0.03	-0.15 ± 0.03	$13/2^+ \to 9/2^+$
663.2	17	0.32 ± 0.05	-0.16 ± 0.06	$19/2^- \to 15/2^-$
707.7	25	0.31 ± 0.07	-0.11 ± 0.09	$15/2^+ \to 11/2^+$
780.8	18	0.24 ± 0.05	-0.03 ± 0.07	$17/2^+ \to 13/2^+$

[a] Energies are within 0.3 keV.

[b] All intensities have been normalized to the 496.2-keV line.

[c] The A_2 and A_4 values were difficult to extract from the data because of small peak-to-background ratio.

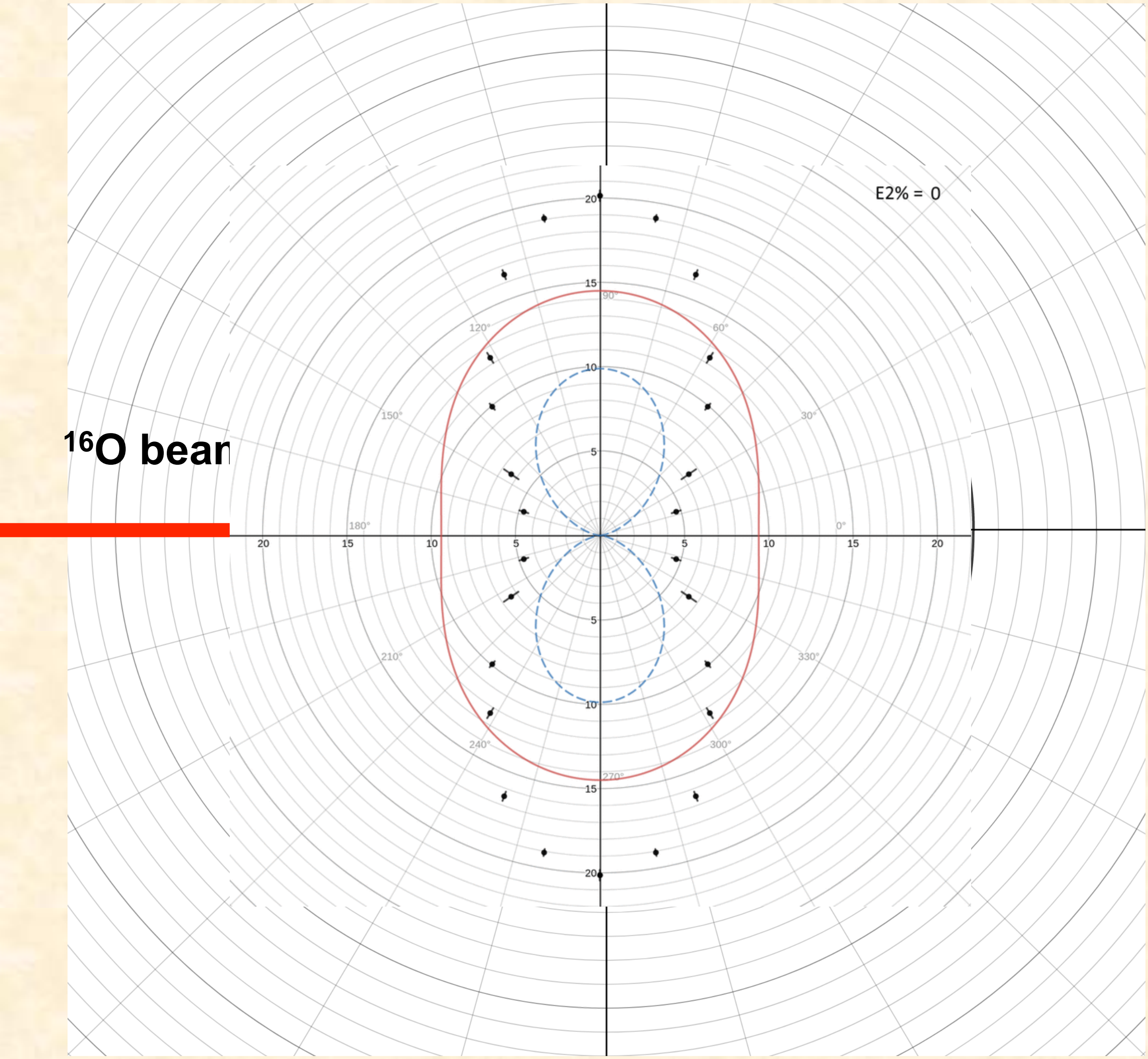

animations courtesy of T. McMaken

◆ Lifetimes

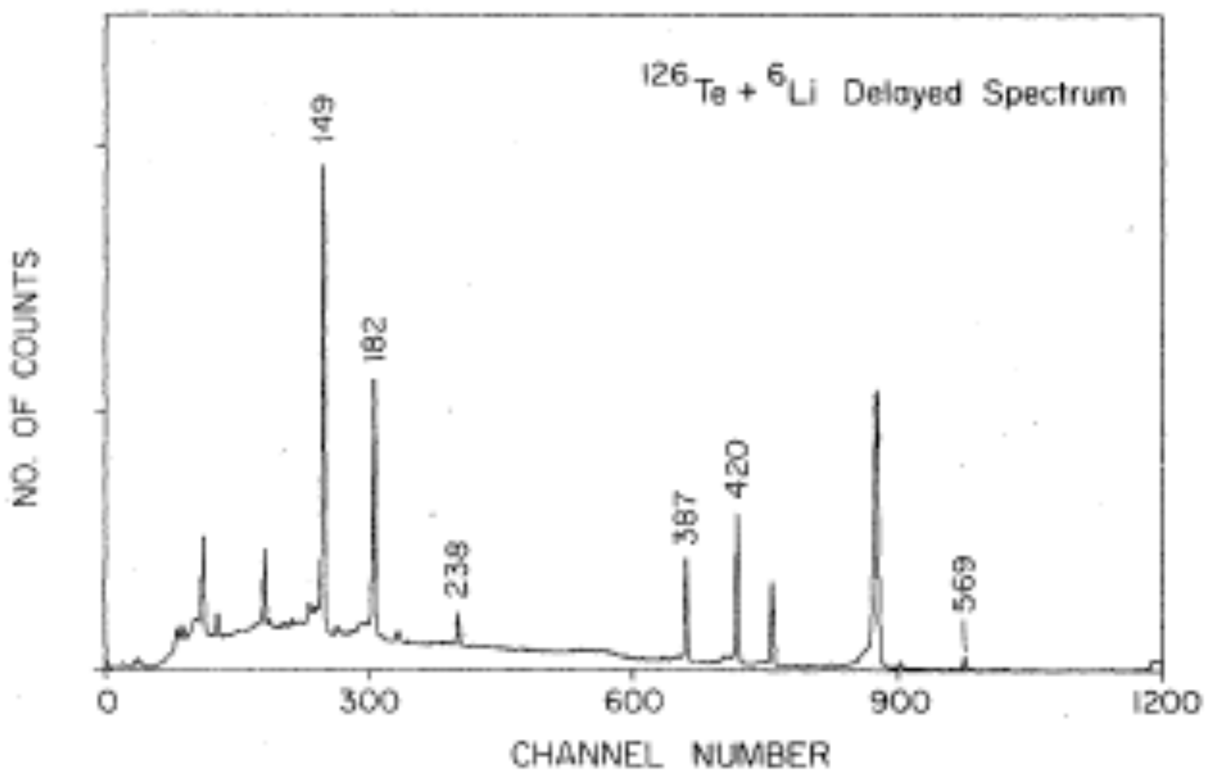

FIG. 3. Delayed γ-ray spectrum for ^{129}Cs obtained from the $^{126}Te(^{6}Li, 3n)^{129}Cs$ reaction. The marked γ-rays cascade decay from the $11/2^-$ isomer.

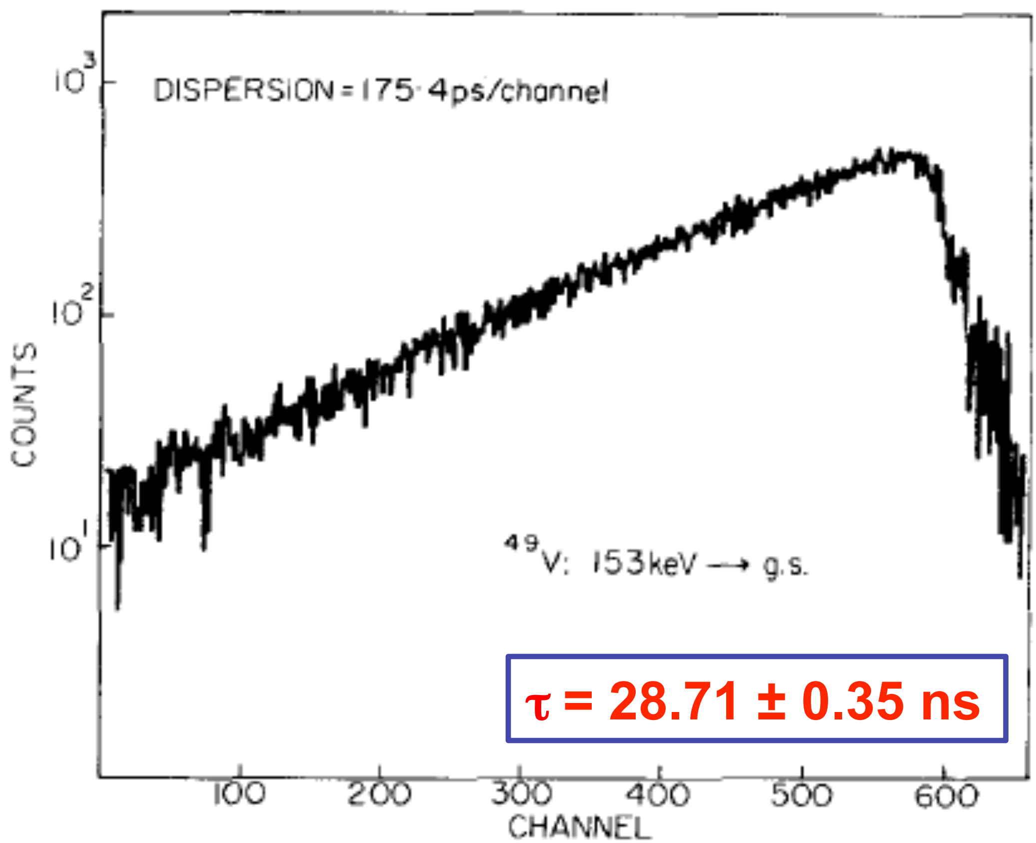

Fig. 5. Delay-time distribution of the 153 keV → g.s. transition in ^{49}V.

1 MHZ pulsing, width <0.5 ns

D.C.S. White *et al.*, Nucl. Phys. A **260**, 189 (1976)

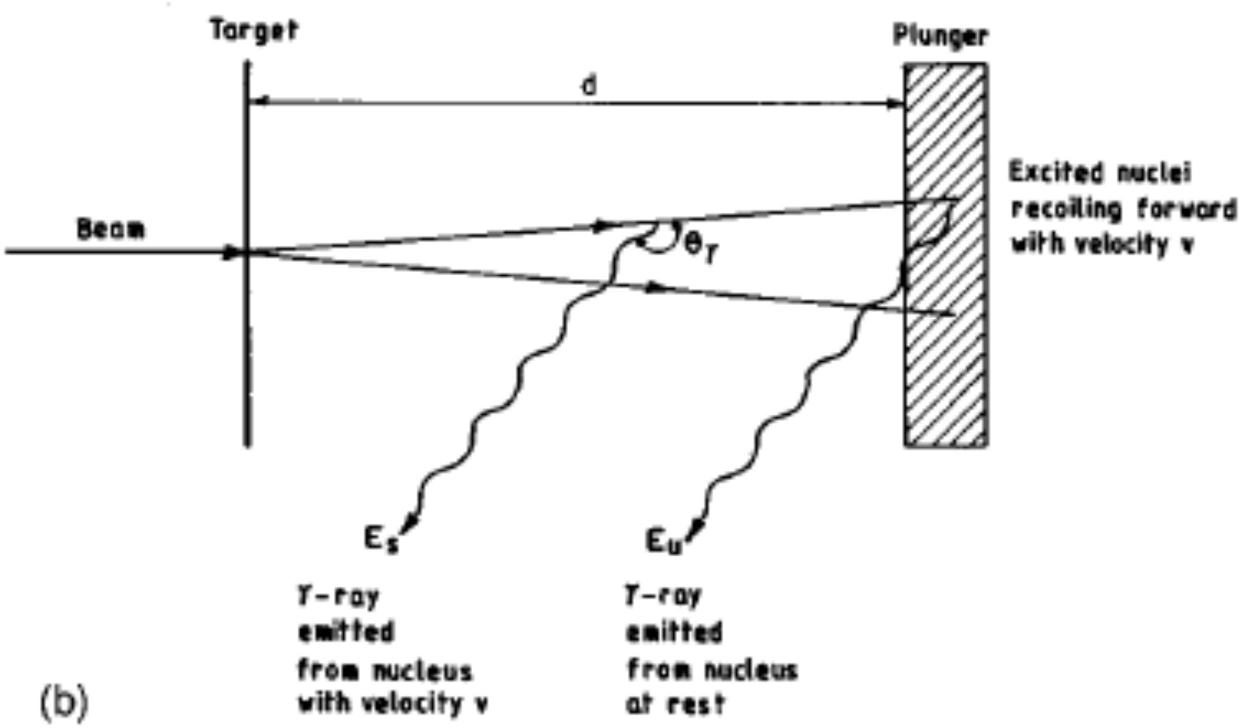

Doppler-Shift Recoil Method

$$R = I_u/(I_s+I_u)$$

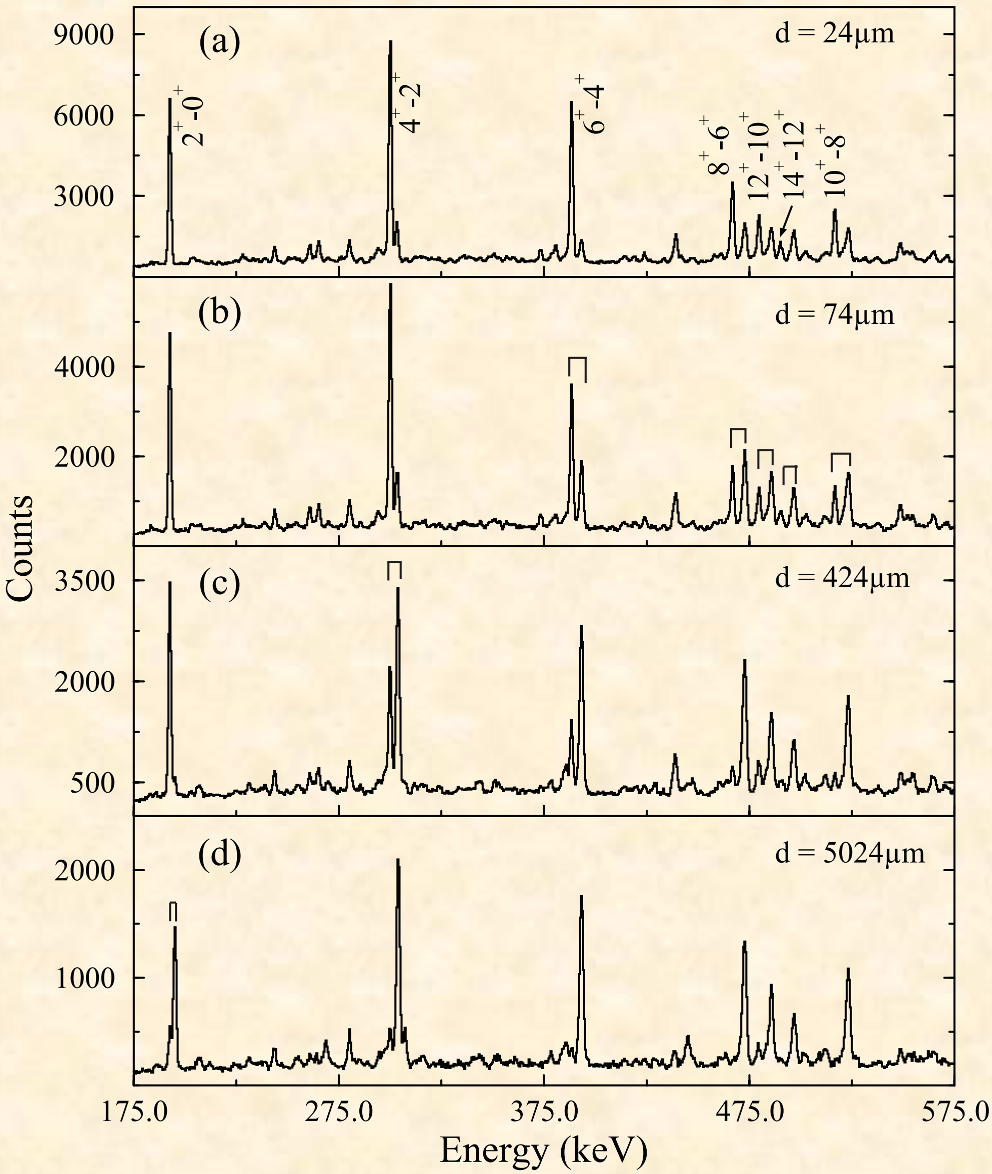

^{186}Pt

J.C. Walpe *et al.*, Phys. Rev. C **85**, 057302 (2012)

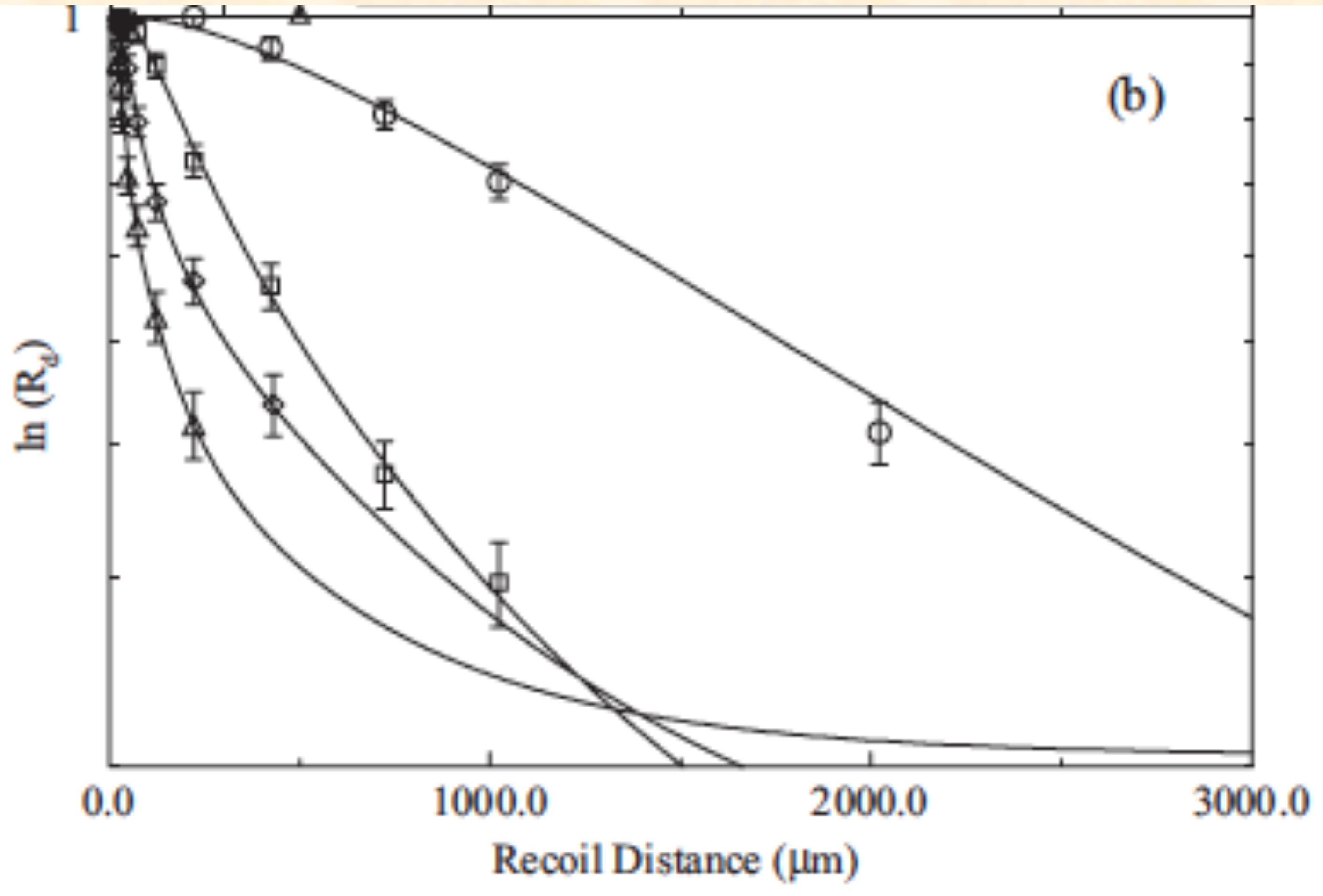

J.C. Walpe *et al.*, Phys. Rev. C **85**, 057302 (2012)

Doppler-Shift Attenuation Method (DSAM)

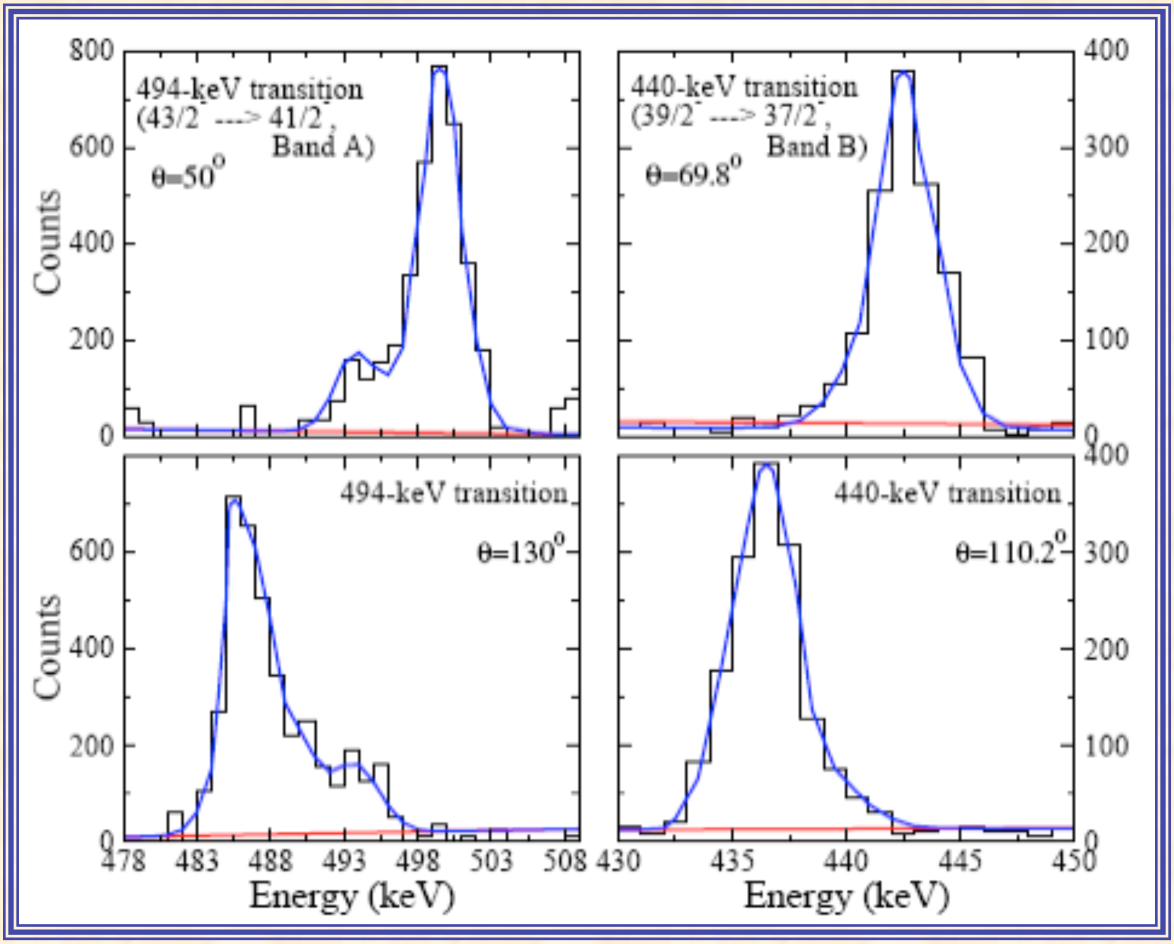

S. Mukhopadhyay *et al.*, Phys. Rev. Lett. **99**, 172501 (2007)

Linear Polarizations

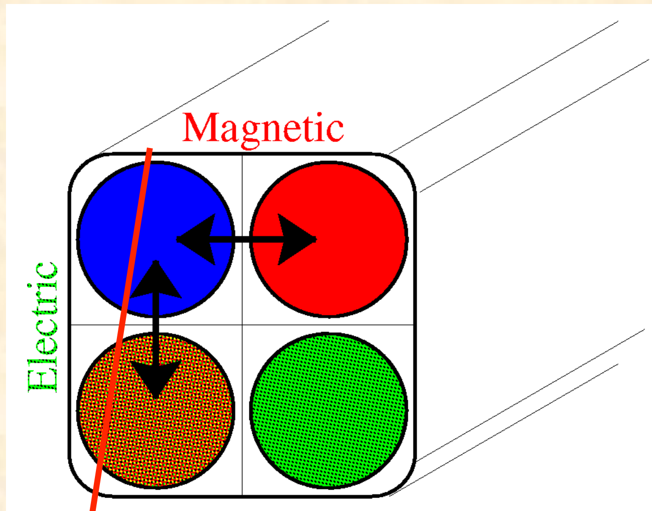

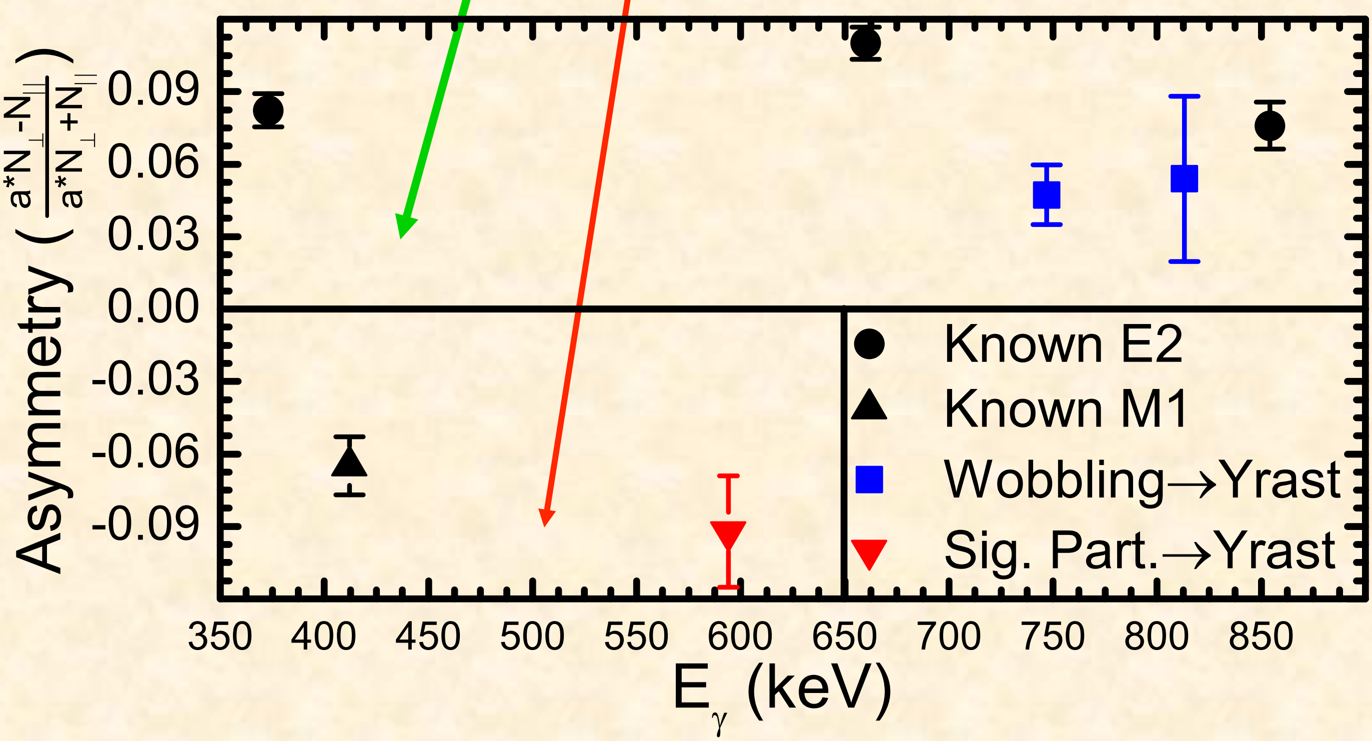

J. T. Matta *et al.*, Phys. Rev. Lett. **114**, 082501 (2015)

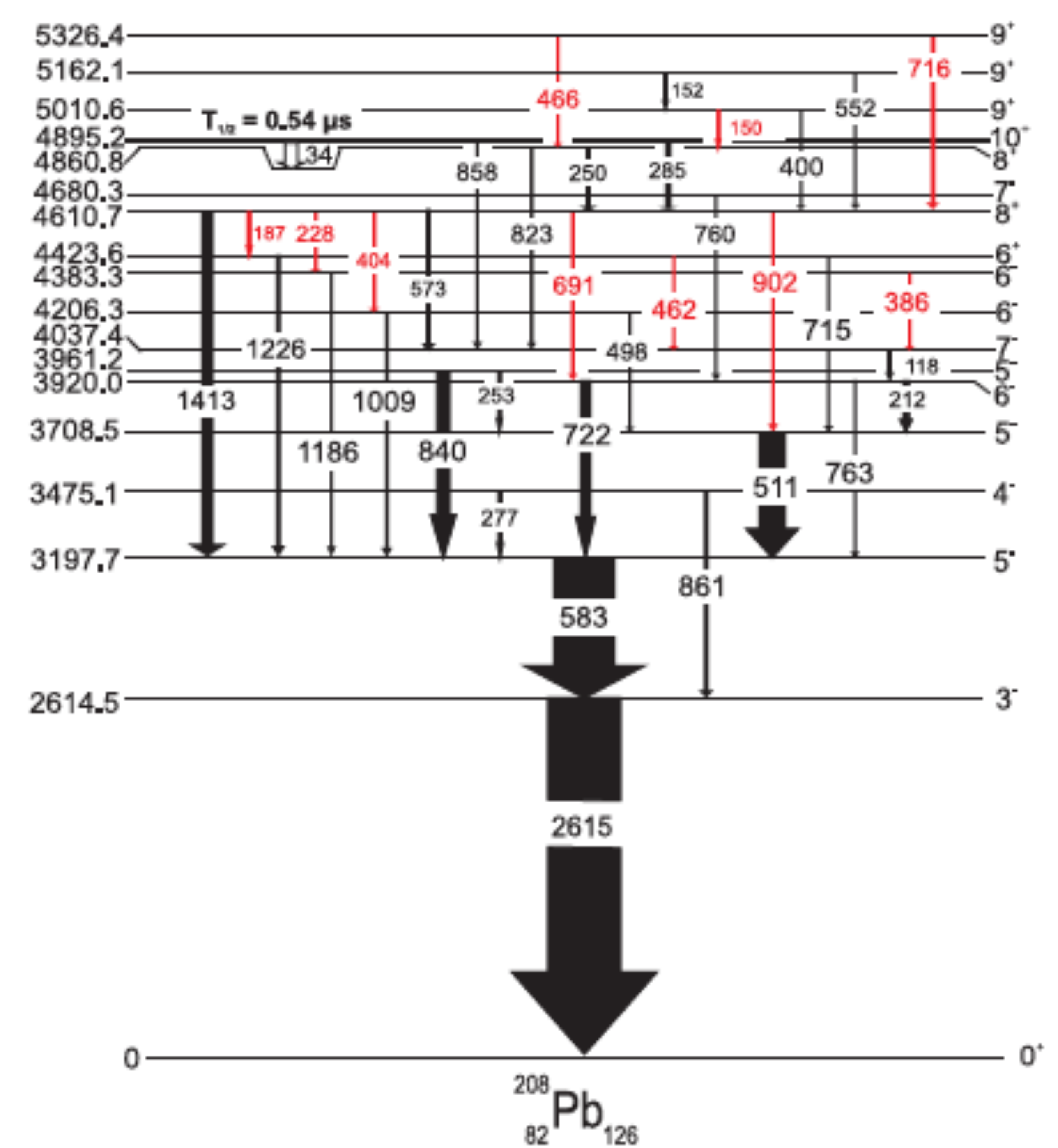

R. Broda *et al.*, Phys. Rev. C **95**, 064308 (2017)

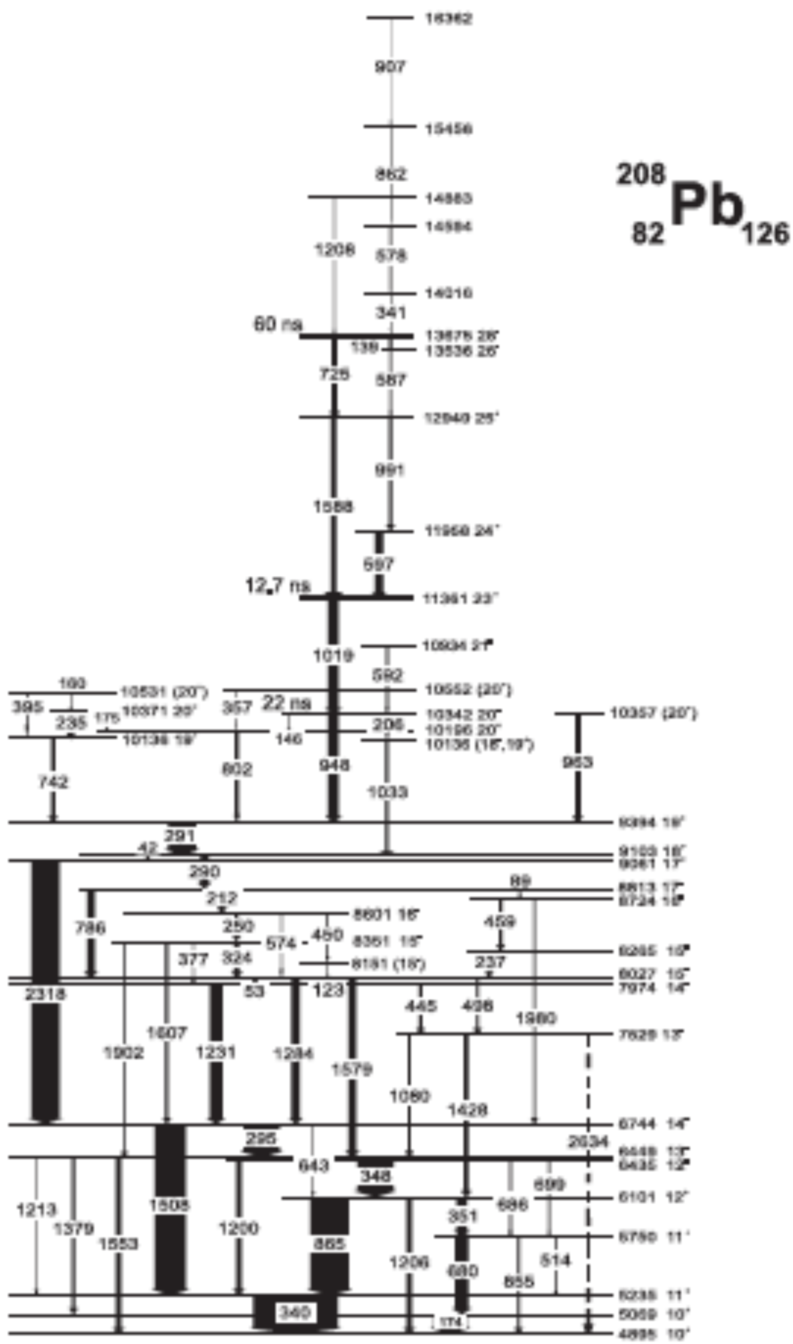

FIG. 4. The ^{208}Pb level scheme including all the states located above the 10^+ isomer established in the present work. The widths of the arrows reflect intensities involved in both prompt and off-beam population. See text for details on the construction of the level scheme and on spin-parity assignments.

Yrast and near-yrast levels up to spin values in excess of I = 30 have been delineated in the doubly magic ^{208}Pb nucleus….

The level scheme was established up to an excitation energy of 16.4 MeV, based on multifold γ –ray coincidence relationships measured with the Gammasphere array.

Large-scale shell-model calculations were performed with two approaches, a first one where the 1, 2, and 3 particle-hole excitations do not mix with one another, and another more complex one, in which such mixing takes place. The calculated levels were compared with the data and a general agreement is observed for most of the ^{208}Pb level scheme. At the highest spins and energies, however, the correspondence between theory and experiment is less satisfactory and the experimental yrast line appears to be more regular than the calculated one.

This regularity is notable when the level energies are plotted versus the I (I + 1) product and the observed, nearly linear, behavior was considered within a simple "rotational" interpretation. Within this approximate picture, the extracted moment of inertia suggests that only the 76 valence nucleons participate in the "rotation" and that the ^{132}Sn spherical core remains inert.

R. Broda *et al.*, Phys. Rev. C **95**, 064308 (2017)

ありがとう

धन्यवाद

Thanks!

The Question Kitten